Microsc. Microanal. 15, 422–434, 2009
doi:10.1017/S1431927609090801

Microscopy AND Microanalysis

The Preimaginal Phases and Development of *Pachycrepoideus vindemmiae* (Hymenoptera, Pteromalidae) on Mediterranean Fruit Fly, *Ceratitis capitata* (Diptera, Tephritidae)

José Tormos,[1,*] Francisco Beitia,[2] Elias A. Böckmann,[1] Josep D. Asís,[1] and Severiano Fernández[1]

[1]*Área de Zoología, Facultad de Biología, Universidad de Salamanca, 37071-Salamanca, Spain*
[2]*Instituto Valenciano de Investigaciones Agrarias, Unidad Asociada de Entomología IVIA/CIB-CSIC, Apartado Oficial, 46113-Montcada, Valencia, Spain*

Abstract: The development and morphology of the immature phases of *Pachycrepoideus vindemmiae* (Rondani, 1875) (Hymenoptera, Pteromalidae) are described from a laboratory rearing culture maintained on *Ceratitis capitata* (Wiedemann, 1824) (Diptera, Tephritidae) using microscopic techniques, including light and scanning electron microscopy. The surface of the chorion of the egg is granulated, and the micropyle occurs at the anterior end. The labrum of the first instar larva does not have sensilla, and the second to fourth instar larvae have setae on the head. The mature larva is characterized by the position and number of the integumental differentations (sensilla and setae). On completion of larval development, an adecticous and exarate pupa is produced. As for the adult, the mandibles of the pupae are toothed. Five larval instars are recorded, based on statistical analyses of the sizes of the larval mandibles in combination with characters such as the number of exuviae and excretion of the meconium. Developmental time from egg to adult emergence was ~18–20 days for males and ~21–23 days for females at 21–26°C, 55–85 relative humidity, and a 16L:8D photoperiod. The results show that the eggs and different larval instars of this parasitoid can be unambiguously identified only by scanning electron microscope.

Key words: Pteromalidae, immature phases, scanning electron microscopy, Tephritidae, management purposes

Introduction

Pachycrepoideus vindemmiae (Rondani, 1875) (Hymenoptera, Pteromalidae) is a solitary primary ectoparasitoid of the pupae of several Diptera pests, although its peculiarity as a hyperparasitoid of dipteran and hymenopteran parasitoids is also known; phenomena of superparasitoidism and multiparasitoidism have also been reported.

Currently, together with *Spalangia cameroni* Perkins, 1910 (Hymenoptera, Pteromalidae), it is one of the parasitoids most widely used in the biological control of the housefly *Musca domestica* (Linnaeus, 1758) and the stable fly *Stomoxys calcitrans* (Linnaeus, 1758) (Diptera, Muscidae), species that are harmful in intensive (confined) raising of livestock and birds (Novartis Animal Health Inc., Perkins Ltda.; Protecnet, 2009). In this respect, it is currently being used in countries such as Denmark, the United States, Australia, Costa Rica, and Colombia in inundative releases, reaching parasitoidism rates of 40% (Steenberg et al., 2001; Geden & Hogsette, 2006). In Spain, since 2003 the species has been bred on a semimassive basis, using the mediterranean fruit fly *Ceratitis capitata* (Wiedemann) (Diptera: Tephritidae) as host with the aim of testing its usefulness as a biological weapon against this dipteran.

As indicated above, most studies addressing *P. vindemmiae* have focused on its potential use in the biological control of Diptera pests. Little attention has been paid to its developmental biology (although see Crandell, 1939). Developmental biology studies, including morphological characterization of the preimaginal stages, can be important for the identification of an insect at species level before adult emergence and can simplify quantification of the impact of natural enemies in biological control programs (Bellows & Van Driesche, 1999; Llácer et al., 2005; Onagbola & Fadamiro, 2008). Little is known about larval morphology in pteromalid wasps (Grassberger & Frank, 2003; Rojas-Gómez & Bonet, 2003; Onagbola & Fadamiro, 2008; Tormos et al., 2007). The present study addresses the characterization of the developmental biology and morphology of the preimaginal stages of this species since the characterization and description offered by Crandell (1939) are succinct and lacking in detail. In this study, statistical analysis of morpho-

Received March 4, 2008; accepted May 18, 2009
*Corresponding author. E-mail: tormos@usal.es

logical parameters, including measurements of the width of the head capsule and mandible length, were used in conjunction with reliable characters, such as the presence of exuvia, excretion of the meconium, and the initiation of the prepupal period, to determine the number of larval instars produced by this parasitoid (Muesebeck & Parker, 1933; Wright, 1986; Löhr et al., 1989; Llácer et al., 2005; Onagbola & Fadamiro, 2008).

Materials and Methods

Insects

The stages of the preimaginal phases and data on the developmental biology of *P. vindemmiae* were obtained from rearing of this parasitoid carried out at the installations of the Instituto Valenciano de Investigaciones Agrarias (IVIA, Valencia, Spain) in a climatic chamber (Sanyo MLR350) at 21–26°C, 55–85% relative humidity (RH), and a 16L:8D photoperiod. In the rearing, pupae of the mediterranean fruit fly were used as hosts, and the parasitoid, confined in a plastic cage (30 × 20 × 20 cm) with ventilation, were fed with honey impregnated on strips of blotting paper, plus sugar and water. These conditions were used throughout the study, with the exception of an RH of 95%, which was used (following the work of Gerling & Legner, 1968 in *S. cameroni*) in the experiments performed to determine the moment of eclosion and the presence of different moults.

Development, Morphology, and Characterization of the Preimaginal Stages

To study the development of the immature stages, ten recently parasitized pupae of *C. capitata* were opened in such a way as to expose the eggs and were placed in a chamber with 95% RH. Periodic observations, four per day (every 6 h), were made of development through the eclosion and exuviae. The slowing down of movement and expulsion of the meconium were used to determine the start of the prepupal period. The pupal phase was considered to be that extending from the transformation of the prepupa in the pupa to the emergence of the adults.

To study the morphology of the immature stages, 15 pairs of parasitoids of 8 days of age taken from a terrarium where large numbers of females and males had cohabited for those eight days were placed individually in a Petri dish (9 × 1.5 cm) and provided daily, until the appearance of the first parasitoid pupae, with ten pupae of *C. capitata* of two days of age [optimum conditions to obtain a good solitary parasitoidism in other species of Pteromalidae (Tormos et al., 2009)]. The parasitized pupae were periodically dissected every 24 h to check the morphological differences of the different stages. To determine the volume of the eggs, the mathematic expression $Vh = 1/6\ (a \cdot b2 \cdot \pi)$ was used; this is commonly employed in the determination of this dimension in ovoid arthropod eggs (Corey & Reid, 1991).

Two hundred eggs, 400 immature larvae, 200 mature larvae, and 200 pupae of *P. vindemmiae* were fixed and preserved in 70% ETOH for subsequent study and description. The ensuing descriptions essentially employ the terminology and organization used by Finlaysson (1987) and Tormos et al. (2004). Voucher specimens are deposited at the IVIA (Valencia, Spain).

Histological Methods, Stereomicroscope, and Scanning Electron Microscope

To prepare the eggs and larval stages for light microscopic, the methods of Tormos et al. (2003, 2004) were employed. Photos and measurements to the nearest 0.01 mm of different structures of the preimaginal phases were taken under a LeicaMZ125 microscope equipped with a Cannon S50 camera using the IM50 Leica software (Leica Microsystems Imaging Solutions). For scanning electron microscopy, the samples were frozen in slush N_2 and attached to the specimen holder of a CT-1500C cryotransfer system (Oxford Instruments, Oxford, U.K.) interfaced with a JEOL JSM-5410 scanning electron microscope (SEM). The samples were then transferred from the cryostage to the microscope sample stage, where the condensed surface water was sublimed by controlled warming to −90°C. Then, the samples were transferred again to the cryostage and sputter-coated with gold. Finally, the samples were returned to the microscope sample stages for visualization at an accelerating voltage of 15 keV. Images were also taken using INCA software of Oxford Instruments.

Statistical Analyses

With the aim of detecting a possible relationship between the length of the mandibles (maximum length: measured from the point of articulation with the head to the pointed tip), and the days of development, both variables were plotted. The linear relationship between both variables was elucidated by fitting a straight line. The same procedure was followed between the width of the head capsule (maximum width) and the time of development, and between the length of the mandibles and the width of the head capsule. Additionally, the same data were also subjected to linear regression analysis to estimate the regression coefficients. Data were tested for normality prior to analysis.

The different groupings of the mandible and head capsule sizes with respect to the time of development obtained with the previous analysis were combined with reliable characters, such as the number of exuviae on the body of the parasitoid larvae and the excretion of the meconium, in order to establish the time of development of the different immature stages and the number of larval instars.

Finally, to determine the possible underlying implicit grouping in the larval instars—with respect to head width

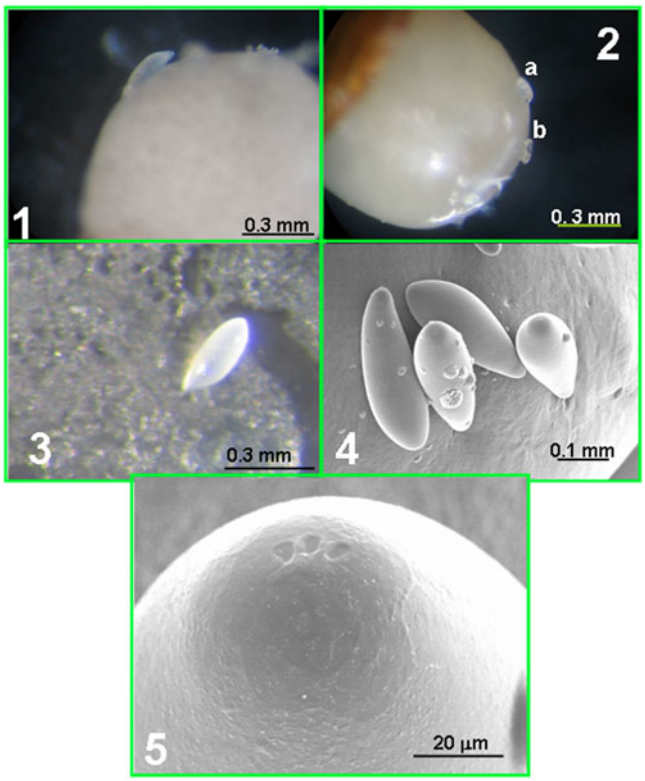

Figure 1–5. *Pachycrepoideus vindemmiae* (Rondani). Egg (under SEM): **1:** Egg on host pupa. **2:** Egg prior to hatching (a) and desiccated egg (b), showing the traslucent chorion on the host pupa. **3:** Egg prior to hatching (detail). **4:** Egg showing the micropylar area (m) at the anterior end. **5:** Detail of micropylar area with the micropyle (m) and the granulate surface of the egg.

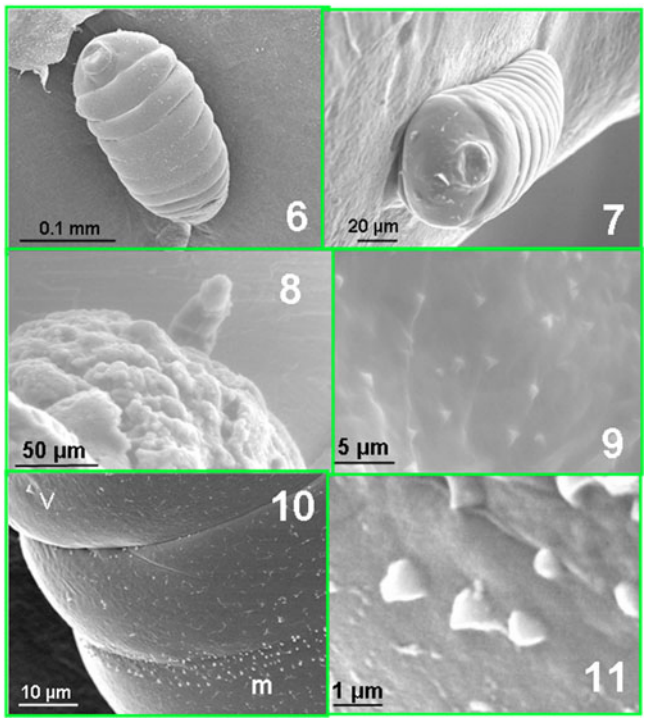

Figure 6–11. *Pachycrepoideus vindemmiae* (Rondani). Larval phase. First instar (under SEM): **6–7:** ventral view (**6**) and frontal view (**7**). **8:** Detail of last segment with cauda. **9:** Detail of the tegument with spinules. **10:** Microtrichiae (m) of the border of segments and ventral setae (s). **11:** Detail of microtrichiae.

and mandible length—a cluster analysis was performed using the hierarchical clustering method. The statistical analysis was performed using the SPSS (12.0) package.

Results

Description and Characterization of the Preimaginal Stages of *P. vindemmiae*

Egg

The egg (Figs. 1–5) [length = 0.21–0.33 mm ($\bar{x} \pm$ SE = 0.27 ± 0.004), maximum width = 0.07–0.12 mm ($\bar{x} \pm$ SE = 0.09 ± 0.01, n = 72)] is waxy white, oval, more or less cylindrical (hymenopteriform), has pointed anterior and posterior tips (Fig. 1), being pointed at only one end and practically rounded at the other prior to hatching (stalked type) (Figs. 2a, 3), with a smooth surface under the stereomicroscope (Fig. 2b). Under SEM, the surface of the corion appears more or less granulate (Fig. 5) and a mycropilar pigmented area with the micropyle (Figs. 4, 5) can be seen at the anterior end of the egg. Although the eggs change shape slightly prior to hatching (change from the hymenopteriform to the stalked type), as may be deduced from a comparison of the volume of 72 specimens [36 of 24 h of age/36 of 48 h of age (prior to hatching)] that the eggs do not increase their size ($F = 0.114$, $df = 1$, $P \geq 0, 736$).

Larva, 1st Instar

General aspect (Figs. 6–7). *Body* [length = 0.25–0.52 mm ($\bar{x} \pm$ SE = 0.37 ± 0.09, n = 12), width (at the level of the prothoracic segment): 0.11–0.32 mm ($\bar{x} \pm$ SE = 0.18 ± 0.08, n = 12)] (Table 1) weakly broader in anterior region, more or less conical in shape (Fig. 7), with defined head capsule and 13 body segments, with the prothoracic segment slightly the widest and the remaining segments narrowing posteriorly, vermiform, whitish, translucent. The neonate larva (Fig. 8) is caudate during the first hours of life. Spiracles (Figs. 14, 18) apparent on the second thoracic segment and three abdominal segments, although nonfunctional spiracles probably appear on first thoracic segment (Fig. 13) and fourth abdominal segment (Fig. 20). Dorsally, laterally, and ventrally (Figs. 12, 17, 20), each segment, except the apical one, bears two pairs of small setae. Additionally, the anterior border of each segment is encircled by a series of microtrichiae (Figs. 10, 11), and the tegument of

Table 1. Measurements (mean ± SE, in mm) of the Body Sizes of the Larval Instars and Pupa of *P. vindemmiae* at Specific Intervals after Parasitization [mature larva: fifth instar (days 10–13) + prepupa (day 14)].

Age (days) after	First Instar		Second Instar		Third Instar		Fourth instar		Fifth Instar		Pupa	
	Length	Width	Length	Width	Length	Width	Length	Width	Length	Width	Length	
parasitoidism	*N* (mean ± SE)	(mean ± SE)	*N* (mean ± SE)	(mean ± SE)	*N* (mean ± SE)	(mean ± SE)	*N* (mean ± SE)	(mean ± SE)	*N* (mean ± SE)	(mean ± SE)	*N*	(mean ± SE)
3	8 0.31 ± 0.04	0.12 ± 0.00										
4	4 0.50 ± 0.01	0.30 ± 0.01	7 0.87 ± 0.19	0.40 ± 0.10								
5			3 1.41 ± 0.21	0.64 ± 0.06	3 1.01 ± 0.04	0.54 ± 0.10						
6					13 2.07 ± 0.68	0.87 ± 0.28						
7					2 2.82 ± 0.30	1.12 ± 0.07						
8							3 2.83 ± 0.29	1.18 ± 0.10				
9							3 2.93 ± 0.30	1.15 ± 0.08				
10									2 2.69 ± 0.64	1.25 ± 0.12		
11									3 3.12 ± 0.19	1.28 ± 0.13		
12									7 3.11 ± 0.16	1.27 ± 0.10		
13									2 3.15 ± 0.14	1.17 ± 0.10		
14									5 2.85 ± 0.12	0.85 ± 0.15		
15–20											28(♂♂)	1.92 ± 0.21
20–23											23(♀♀)	1.70 ± 0.30

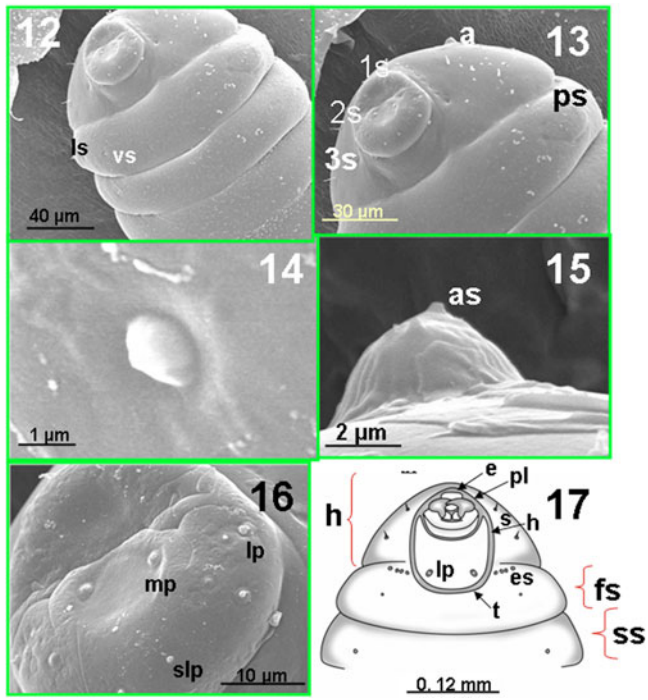

Figure 12–17. *Pachycrepoideus vindemmiae* (Rondani). Larval phase. First instar (under SEM): **12–13:** Ventral view of the head and anterior segments of the body showing the circular structure (**12**, cs) that surrounds the mouthparts, and detail (**13**) of the antenna (a), setae of the head capsule (first pair, 1s; second pair, 2s; third pair, 3s) and situation of prothoracic spiracle (ps) and lateral (ls) and ventral setae (vs) of the body. **14:** Detail of the prothoracic spiracle. **15:** Antenna showing a detail of apical sensilla (as). **16:** Detail of the circular structure surrounding the mouthparts, showing the possible labial palpi (lp) and sensilla (slp) arranged behind them, together with the possible maxillary palpi (mp). **17:** First instar (figure): head (h), first (fs), and second (ss) thoracic segments in ventral view showing mandibles (m); setae (s) and other sensory structures (es), among which striking are the possible labial palpi (pl) with two sensilla; structures of the cephalic skeleton: epistoma (e), pleurostoma (pl), hypostoma (h), and tentorium (t).

different zones of the body in the ventral part shows very minute spinules (Fig. 9). Last abdominal segment notched transversely (Fig. 22). *Cranium* (Figs. 6, 7, 12, 13, 16) [width = 80–90 mm ($\bar{x}$ ± SE = 85 ± 2.79, n = 12)] (Table 2) with the cephalic skeleton well developed (Fig. 16), showing as well the tentorium, the following sclerites distinct and sclerotized: epistoma, pleurostoma—with superior and inferior mandibular processes—and hypostoma. It has a prominent more or less tubular/circular structure formed from the integument and surrounded the mouthparts (Figs. 12, 13). Around this structure there are three pairs of setae (Figs. 12, 13, 21) and two papilliform antennae with two apical sensilla (Figs. 14, 15, 21, 23). *Mouthparts*: Mandibles (Fig. 16) [length = 12–13 μm ($\bar{x}$ ± SE = 12.50 ± 0.52, n = 10)] (Table 2) well defined, with an oblong molar

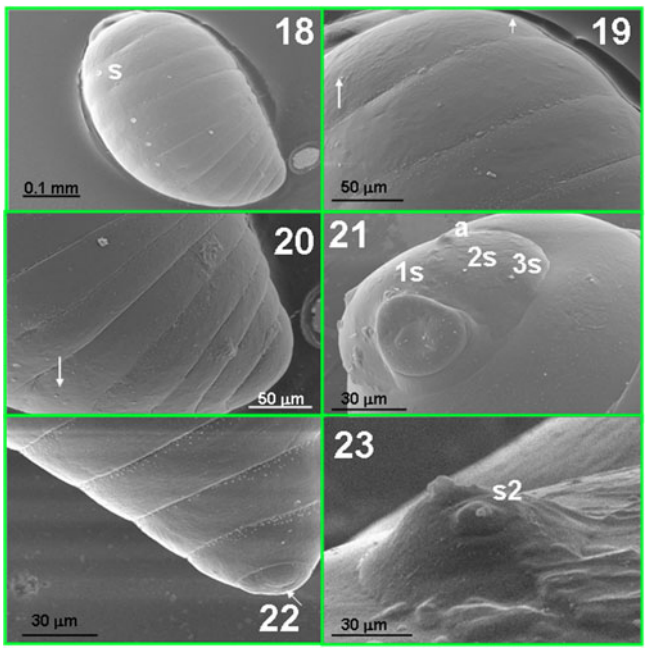

Figure 18–23. *Pachycrepoideus vindemmiae* (Rondani). Larval phase. First instar (under SEM): **18:** Dorsal view showing the spiracles (s). **19:** First segment of the body showing the distribution of the setae in dorsal part. **20:** Last segments of the body showing (see arrow) a probable nonfunctional spiracle. **21:** Anterior part of the body, showing a detail of antennae (a) and distribution of setae (1s, 2s, 3s) of the head. **22:** Last abdominal segment notched transversely (see arrow). **23:** Antenna showing the sensilla on apex.

lobe and one sharp blade, slightly curved, and well sclerotized. Maxillae and labium indistinguishable, although in Figures 16 and 17 it is possible to observe sensory structures that could correspond to labial palpi (a), maxillary palpi (b), and sensilla arranged behind labial palpi. This instar lasts for ≈2 days. These larvae are only mobile just after hatching because after a few hours they lose their tail and become fixed on the host. Using their mandibles, they perforate it and feed on it. They may change locations several times. At the end of this period, the larvae averaged 0.50 ± 0.01 mm in length and 0.30 ± 0.01 mm in width (Table 1).

Larva, 2nd Instar

General aspect (Fig. 24). *Body* [length = 0.69–1.57 mm ($\bar{x}$ ± SE = 1.03 ± 0.32, n = 10), width (at the level of the mesothoracic segment): 0.31–0.69 mm ($\bar{x}$ ± SE = 0.47 ± 0.14, n = 10)] (Table 1) similar to the first instar larva, although with the following particularities: (a) prothoracic segment with numerous papillae (Fig. 25)—probably with a sensory function—in the pleural area; (b) functional spiracles on metathoracic segment (Figs. 25, 26), although the mesothoracic ones are larger (Fig. 25); (c) absence of a circular structure surrounded the moutparts (Fig. 27); (d) an-

Table 2. Length of the Mandible and Width of the Head Capsule (both in µm) of the Larval Instars of *P. vindemmiae* at Specific Intervals after Parasitization [mature larva: fifth instar (days 10–13) + prepupa (day 14)]. Intervals of Presence of Pupae ♂♂ (days 18–20) and ♀♀ (days 18–23).

Age (days) after	First Instar			Second Instar			Third Instar			Fourth Instar			Fifth Instar			Pupae	
	Width		Length	Width		Length	Width		Length	Width		Length	Width		Length		
parasitoidism	*N*	(mean ± SE)	*N*	(mean ± SE)	*N*	(mean ± SE)	*N*	(mean ± SE)	*N*	(mean ± SE)	*N*	(mean ± SE)	*N*	(mean ± SE)	*N*	*N* ♂♂	♀♀
3	8	83.87 ± 1.88	8	12.37 ± 0.51													
4	4	87.25 ± 3.20	2	13.00 ± 0.00	7	290.28 ± 12.33	7	20.85 ± 1.05									
5					3	310.00 ± 0.00	3	22.00 ± 0.00	3	340.00 ± 0.00	3	28.00 ± 0.00					
6									13	345.38 ± 5.18	13	28.76 ± 0.43					
7									6	351.66 ± 2.58	6	29.00 ± 0.00					
8											3	351.66 ± 2.88	3	40.33 ± 0.57			
9											3	353.33 ± 2.88	3	40.66 ± 0.57			
10													2	355.00 ± 0.00	2	50.00 ± 0.00	
11													3	355.00 ± 0.00	3	51.00 ± 0.00	
12													7	353.57 ± 3.77	7	51.14 ± 1.06	
13–14													7	357.50 ± 3.53	2	51.00 ± 0.00	
15–18																	51
18–20																28	
20–23																	23

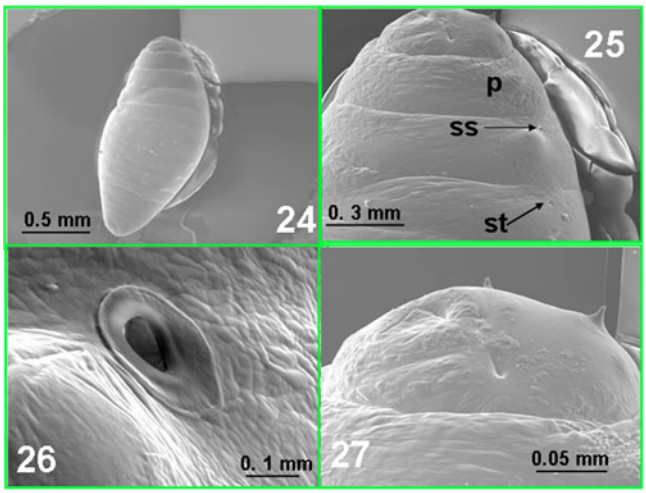

Figure 24–27. *Pachycrepoideus vindemmiae* (Rondani). Larval phase. Second instar (under SEM): **24:** General aspect in dorsal view. **25:** Anterior segments of the body showing the mesothoracic (ss) and metathoracic (st) spiracles (note difference in size) and papillae (p) in prothoracic segment. **26:** Detail of metathoracic spiracle. **27:** Detail of mouthparts.

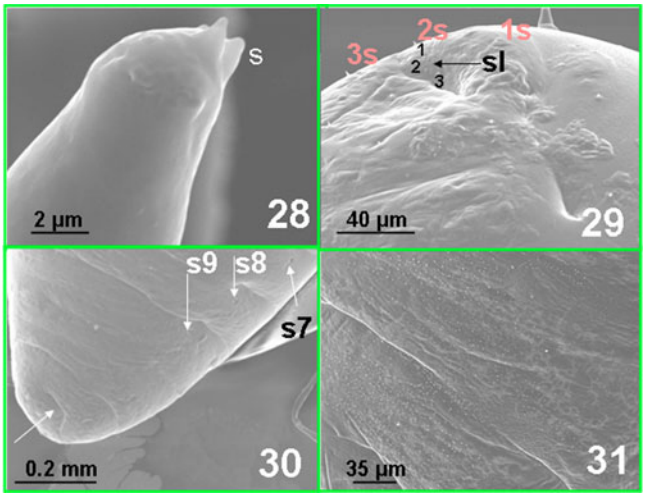

Figure 28–31. *Pachycrepoideus vindemmiae* (Rondani). Larval phase. Second instar (under SEM): **28:** Antenna (s, sensillum). **29:** Detail of the distribution of tegumental differentations of labrum: (a) setae (1s–3s), (b) sensilla of labrum (1–3). **30:** Last abdominal segments showing spiracles 8–9 (s8–s9) as well as the slit of the last abdominal segment. **31:** Detail of the microspinulose surface of the last abdominal segment.

tennae more developed, longer (Fig. 28); (e) labrum with three sensilla (Fig. 29); (f) nine pairs of spiracles (Fig. 30); and (f) last abdominal segment almost completely spinulose (Fig. 31). Additionally, the head is wider (width = 280–310 μm, $\bar{x} \pm$ SE = 296.20 ± 13.86, n = 10) and the blade of mandibles is almost straight, with sharp and heavily sclero-

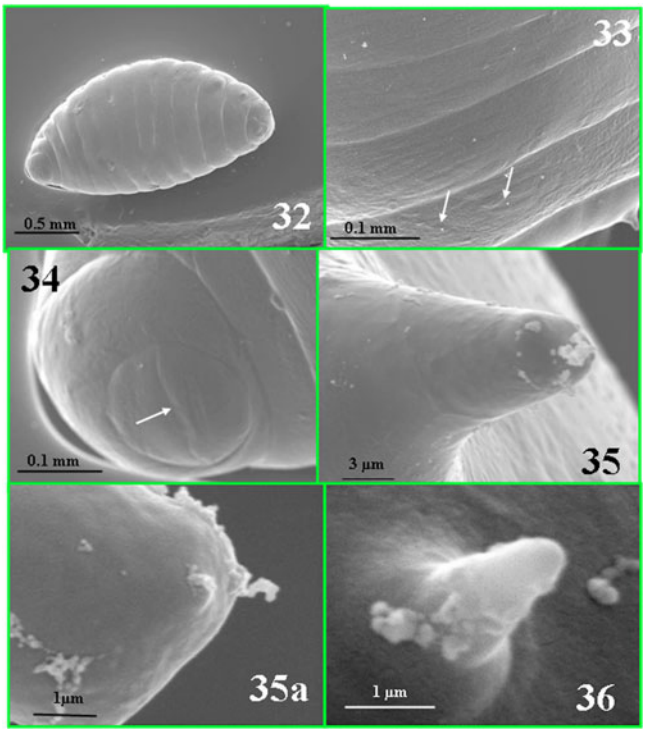

Figure 32–36. *Pachycrepoideus vindemmiae* (Rondani). Larval phase. Third instar (under SEM): **32:** General aspect in lateral view. **33:** Anterior part of the body in dorsal view showing the distribution of setae (see arrow). **34:** Detail of last segment of the body showing the transversal slit (see arrow). **35:** Antenna showing the barely protruding apical sensilla (see detail Fig. 35a). **36:** Detail of seta of the clypeo-labral structure.

tized tips, and the mandible has the greatest length (length = 20–22 μm, $\bar{x} \pm$ SE = 21.20 ± 1.03, n = 10). The presence/absence, type, and distribution of the tegumental differentations of the head (Fig. 29) is more similar to that of the first instar larva. The last abdominal segment is also notched (Fig. 30). This instar lasts for ≈1.5 days. At the end of this period, the larvae averaged 1.41 ± 0.21 mm in length and 0.64 ± 0.06 mm in width (Table 1).

Larva, 3rd Instar

General aspect. *Body* (Fig. 32) [length = 0.96–3.18 mm ($\bar{x} \pm$ SE = 2.13 ± 0.78 mm, n = 21), maximum width = 0.47–1.25 mm ($\bar{x} \pm$ SE = 0.89 ± 0.28, n = 21)] (Table 1) hymenopteriform, with a similar distribution of the setae of the tegument, although with a greater number (Fig. 33), and morphology of the last segment (Fig. 34) to those exhibited by the second instar larva, but with the following differences with respect to the state mentioned, which in turn approximate it to mature larva: (a) antennal sensilla scarcely protruding (Figs. 35, 35a), (b) probable maxillary and labial palpi (Figs. 37, 38) more differentiated, (c) setae of the head more reduced and more numerous (Fig. 39), and (d) setae

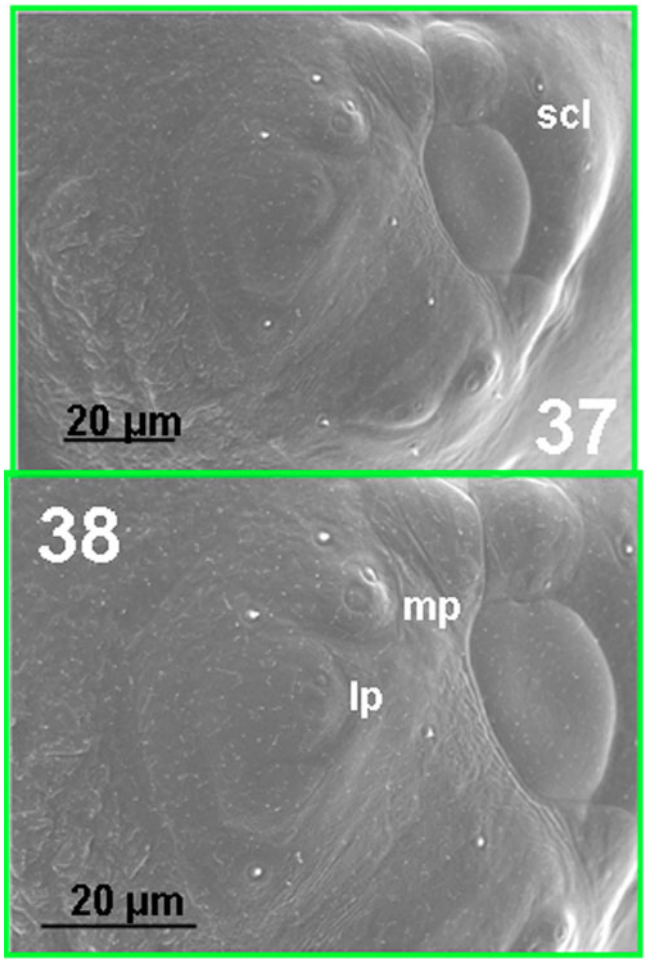

Figure 37–38. *Pachycrepoideus vindemmiae* (Rondani). Larval phase. Third instar (under SEM): **37:** Detail of mouthparts + clypeo-labral structure: scl, clypeo-labral seta. **38:** Detail of mouthparts: mp and lp, probable maxillary and labial palpi, respectively.

on clypeus-labrum structure (Figs. 36, 38). Additionally, unlike of the second instar, this instar has a greater width of the head capsule (width = 340–355 μm, $\bar{x} \pm$ SE = 346.66 ± 5.55, $n = 22$) and the mandibles (length = 28–29 μm, $\bar{x} \pm$ SE = 28.72 ± 0.45, $n = 22$) are longer (Table 2). This instar lasts for ≈2 days. At the end of this period, larvae averaged 2.82 ± 0.30 mm in length and 1.12 ± 0.07 in width (Table 1).

Larva, 4th Instar

General aspect. *Body* [length = 2.50–3.20 mm ($\bar{x} \pm$ SE = 2.88 ± 0.27 mm, $n = 6$), maximum width = 1.05–1.30 mm ($\bar{x} \pm$ SE = 1.16 ± 0.08, $n = 6$)] (Table 1) very similar to the third instar even with respect to the width of the head capsule (width = 350–355 μm, $\bar{x} \pm$ SE = 352.50 ± 2.73, $n = 6$), although with greater mandible length (length = 40–41 μm, $\bar{x} \pm$ SE = 40.50 ± 0.54 μm, $n = 6$) (Table 2). In this instar, the tegument has a large number of concavities

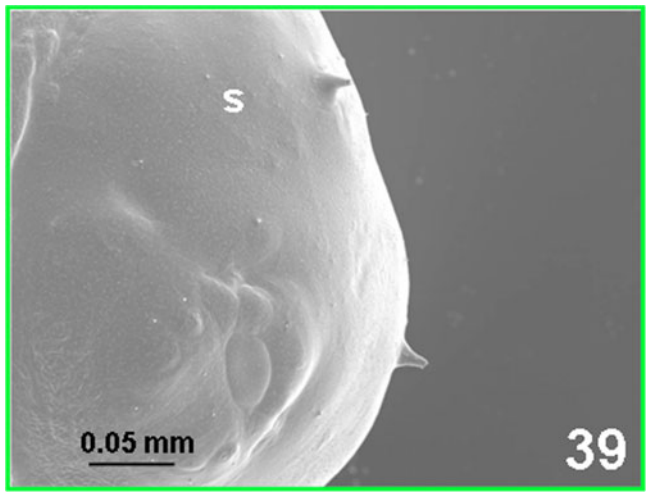

Figure 39. *Pachycrepoideus vindemmiae* (Rondani). Larval phase. Third instar (under SEM): Detail of head showing the distribution of setae: s (seta).

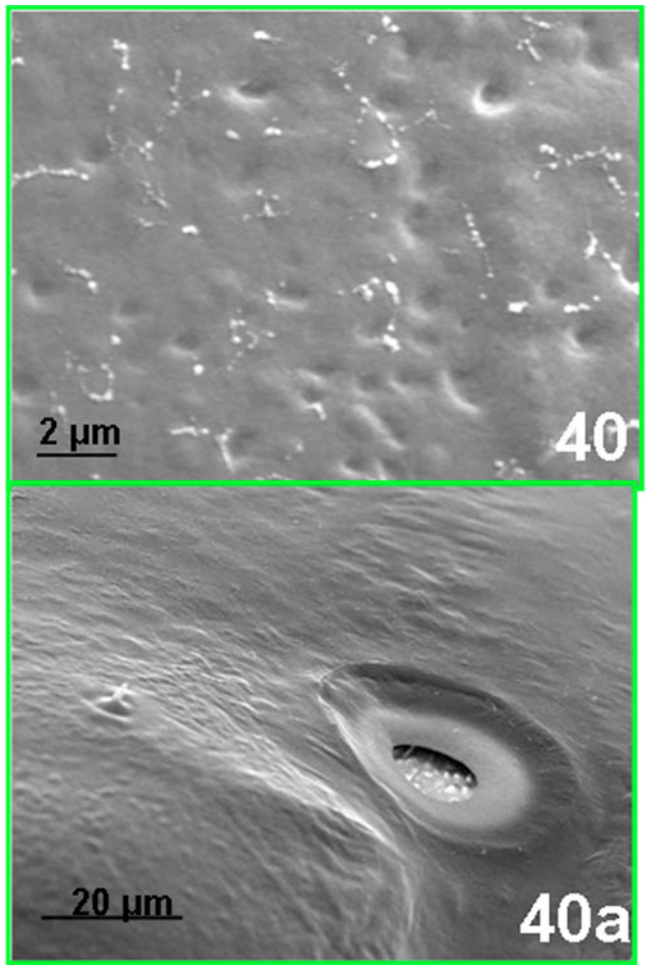

Figure 40–40a. *Pachycrepoideus vindemmiae* (Rondani). Larval phase. Fourth instar (under SEM): **40:** Detail of the tegument. **40a:** Mesothoracic spiracle.

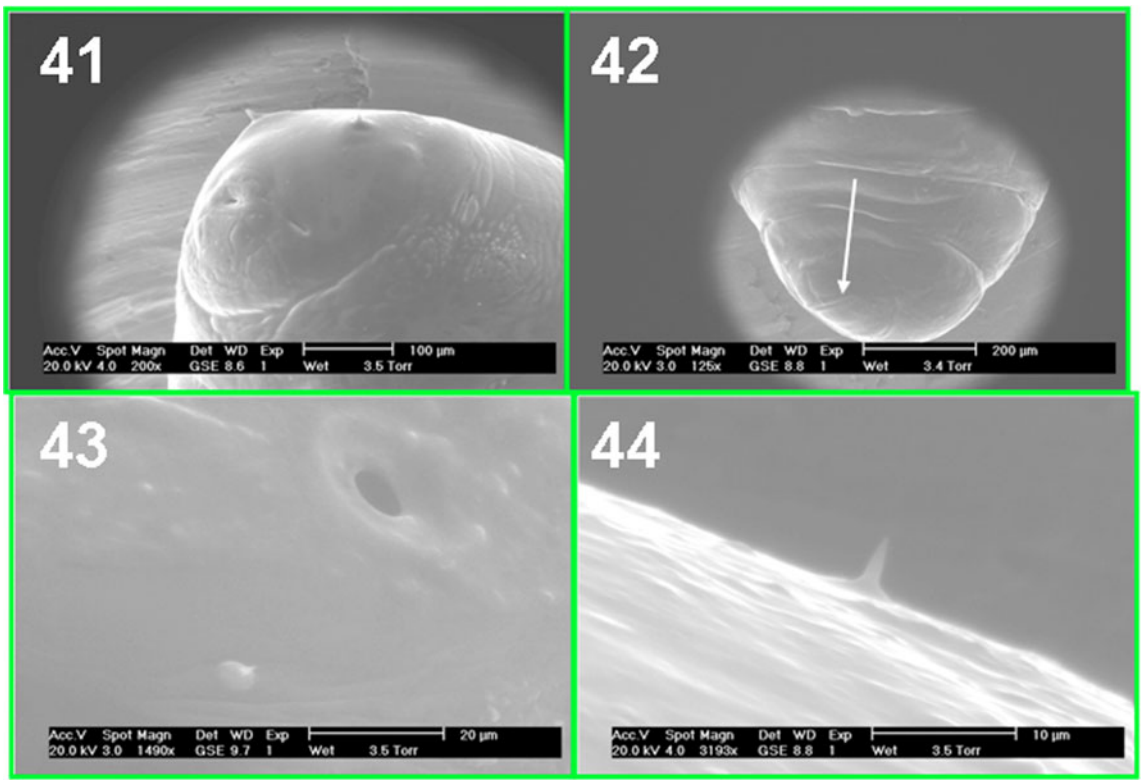

Figure 41–44. *Pachycrepoideus vindemmiae* (Rondani). Larval phase. Fifth instar (mature larva) (under SEM): **41:** Head in lateral view. **42:** Detail of last abdominal segment showing the transversal slit (see arrow). **43:** Detail of spiracle showing a seta, of those present on all segments, close to. **44:** Detail of a seta.

(Fig. 40)—probably sensory structures—and spiracles with the peritreme highly defined (Fig. 40a). This instar lasts for ≈1.5 days. At the end of this period, larvae averaged 2.93 ± 0.30 mm in length and 1.15 ± 0.08 in width (Table 1).

Larva, 5th Instar (Mature Larva)

General aspect. *Body* [length = 2.63–3.30 mm ($\bar{x}$ ± SE = 3.06 ± 0.21 mm, $n = 14$), maximum width = 1.17–1.45 mm ($\bar{x}$ ± SE = 1.25 ± 0.10, $n = 14$)] (Table 1). This instar is very similar to the third and fourth instars (Figs. 41–44) even as regards the width of the head capsule (width = 350–360 μm, $\bar{x}$ ± SE = 354.64 ± 3.07, $n = 14$) (Table 2). Under the light microscope, in this instar it is possible to observe on the head capsule the configuration the cephalic sclerites, which show a marked difference with those of the first instar, as well as one pair of sensilla above and one pair below the preoral cavity (Fig. 45). The spiracles display a subatrium with several well-differentiated chambers (Fig. 46). Nevertheless, the length of the mandibles (length = 50–53 μm, $\bar{x}$ ± SE = 50.92 ± 0.82, $n = 14$) separates this instar from the preceding ones (Table 2). This instar lasts for ≈5 days. At the end of this period (Fig. 47), the larvae averaged 2.85 ± 0.12 in length and 0.85 ± 0.15 in width (Table 1). A reduction in the size of the predefecant mature larva to the prepupa (postdefecant mature larva) was observed (see Table 1; for example, 3.15 ± 0.14 mm in length and 1.17 ± 0.10 in width along the fourth day), probably due to expulsion of the meconium.

Pupa

General aspect (Fig. 48). Naked [length = 1.6–2.00 mm ($\bar{x}$ ± SE = 1.82 ± 0.31 mm, $n = 51$)] (Table 1). Adecticous and exarate. Initially, this immature stage is white but in ≈2 days pigmentation begins to appear until the dark adult coloration is reached. The most outstanding character of this phase lies in the presence of numerous long setae on the vertex of the head (Fig. 49); in contrast, the corresponding area on the larval or adult head is bare. The adults use their mandibles to chew a small irregular circular emergence hole (Fig. 50) through the puparial wall, usually at the anterior end or at the middle part of the puparium. This instar lasts for ≈8 days. The males emerged in ≈4–6 days and the females in ≈6–8 days (Table 2).

Total Developmental Time

Under the above environmental conditions, the eggs of *P. videmniae* hatch into neonate first instar larvae in ≈48 h. The total larval developmental period is ≈12 days under

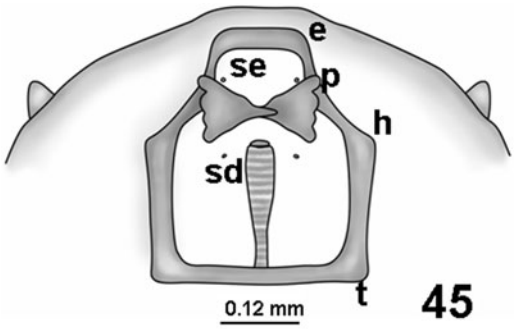

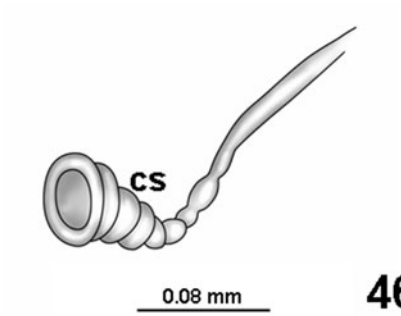

Figure 45–46. *Pachycrepoideus vindemmiae* (Rondani). Larval phase. Fifth instar (mature larva). (Figures obtained with light microscopy.) **45:** Head, in ventral view, showing the configuration of cephalic sclerites (e = epistoma, p = pleurostoma, h = hypostoma, t = tentorium) and sensillae located above (se)/below (sd) the preoral cavity. **46:** Prothoracic spiracle showing detail of chambers of subatrium (cs).

the same conditions (Table 1). Male and female individuals spend ≈6 and 9 days, respectively, as pupae before emergence. Thus, the complete development of male *P. videmniae* lasts 18–20 days, the females emerging up to 3 days later (Table 2).

Characterization and Separation of Immature Stages

The immature stages of *P. videmniae* were separated *a priori*, on the basis of their age, by means of the presence of exuviae and prepupa and the excretion of the meconium. These initial data, taken from an experiment designed specifically to study the development of the immature stages [climatic chamber (Sanyo MLR350) at 21–26°C, 95% RH, and 16L:8D photoperiod], served as a reference to separate the different preimaginal phases and the different larval instars, obtained from parasitized pupae of the offspring (same conditions than before except for the 55–85% RH).

The data relating to the mandible length (obtained from individuals of the offspring) of the larvae (the larvae have simple, tusk-like mandibles—above all the first phase, which has a curved blade while in the other instars it is straight—whereas the mandibles of the pupae and the adults are toothed at the tip) were subjected to a "box-plot" (Fig. 51) and a "scatter plot" (Fig. 52), revealing both effects of age (time period between oviposition and extraction of larva from the host) on the length of the mandibles (m-lengths) of larvae of *P. vindemmiae* of different ages. In particular, using this variable it was possible to separate all larvae into five groups (instar groupings) that were well differentiated (different instars as shown by the previous experiment) (Figs. 51, 52), and a linear relationship was established between mandible length and the time of development (Fig. 52). Subsequent one-way factorial ANOVA revealed significant effects of age (larval instars) on m-length ($F_{4,61}$ = 5,615, 78 $P < 0.001$). An additional Tukey's HSD test revealed significant differences at the 95% confidence level between the pairs of means of five well-differentiated groups (larval instars) (Fig. 51). Finally, linear regression analysis confirmed positive correlations between m-lengths and instar groupings (Fig. 52), suggesting that larval mandible length is a good predictor of the number of larval instars in *P. vindemmiae*. A scatterplot (Fig. 53) did not reveal significant effects of age (larval instar) on the width of the head capsule, and it was not possible to establish a linear relationship between the width of the head and the time of development. As from the second instar, the width of the head remained almost unvaried (Fig. 54). Accordingly, using this variable it is not possible to separate all larvae into five well-delimited groups (instar groupings). The results obtained from these analyses, as well as of the suitable experiment at the beginning of this section, were used to compile Tables 1 and 2. Additionally, a cluster analysis performed with the mandible length variable (Fig. 55) revealed a perfect delineation of five groups, corresponding to the five larval instars shown by the larval phase of *P. vindemmiae*.

Discussion

The data concerning the biology and development of *P. vindemmiae* under the indicated environmental conditions of temperature, photoperiod, and RH, using *C. capitata* as host, are similar to those obtained previously for this parasitoid on *Piophila casei* (Linnaeus, 1758) (Diptera, Piophilidae) (Crandell, 1939).

A character commonly employed to characterize larval instars in parasitoids, such as mandible length (Dyar, 1890; Muesebeck & Parker, 1933; Löhr et al., 1989; Wen et al., 1995; Tschinkel et al., 2003; Llácer et al., 2005; Onagbola & Fadamiro, 2008), allowed us to corroborate the number of larval instars that had been established previously from the presence of the exuviae. Our results show that mandible lengths are positively correlated to instar groupings, suggesting that both may also be reliable as characters for determining the number of instars in parasitoids. Additionally, mandible length has been used in morphometric studies (Kawano, 2000; Manzoor & Akhtar, 2006; Onagbola & Fadamiro, 2008). Nevertheless, the larval instars did not

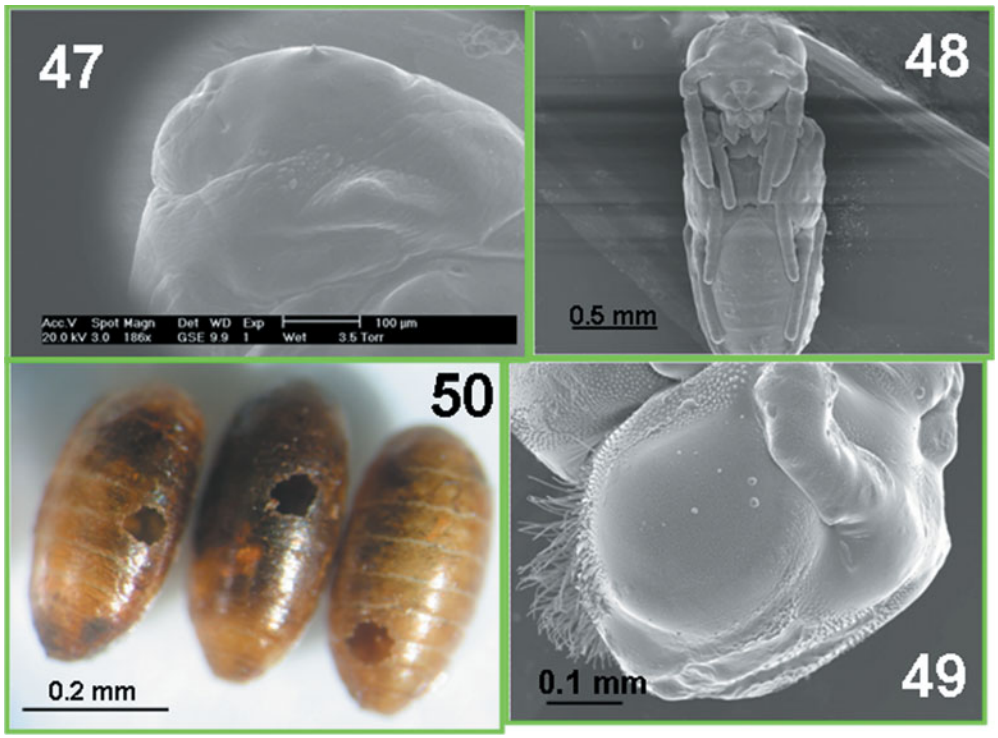

Figure 47–50. *Pachycrepoideus vindemmiae* (Rondani). Larval phase. Fifth instar (postdefecant mature larva, prepupa) (under SEM): **47:** Head in lateral view. Phase of pupa (under SEM): **48:** Pupa in ventral view. **49:** Head showing a cushion on vertex composed of numerous long setae. Puparia of host (under microscope): **50:** Puparia de *C. capitata* showing the emergency holes of *P. vindemmiae*.

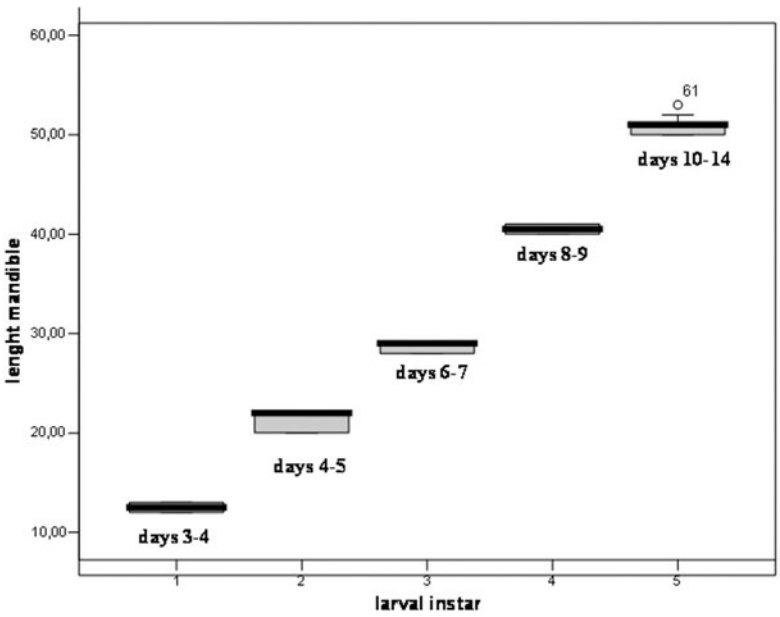

Figure 51. Box-plot showing box diagrams representing the median, quartiles, and upper and lower whiskers of mandible length as a function of the larval instar in question.

reveal significant effects of age on the width of the head capsule, and it is not possible to establish a linear relationship between the width of the head and the time of development. As from the second instar, head width remains practically unmodified. This has been reported for other Chalcidoidea, although the number of larval instars produced by an insect species has usually been determined by measuring the widths of the head capsules of the larvae

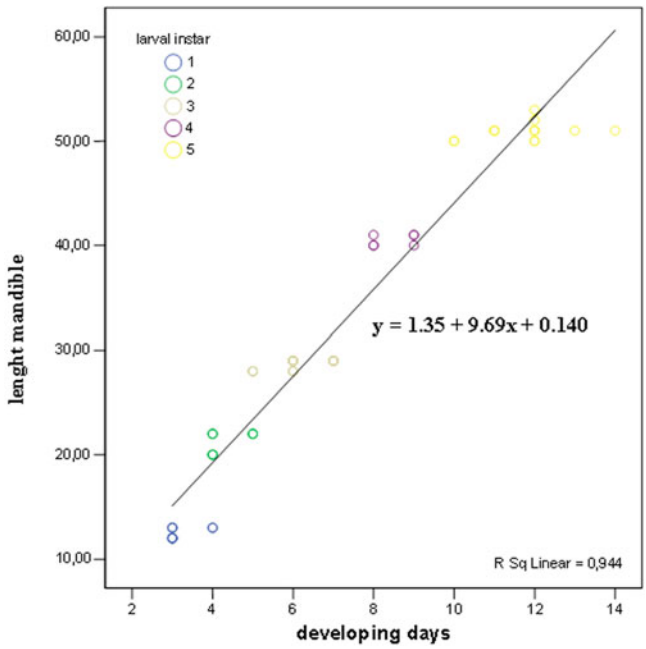

Figure 52. Scatter plot showing the relationship between the length of the mandibles, larval age, and larval instar [the fifth larva is the mature larva: predefecant mature larva + postdefecant mature larva postdefecant (prepupa)].

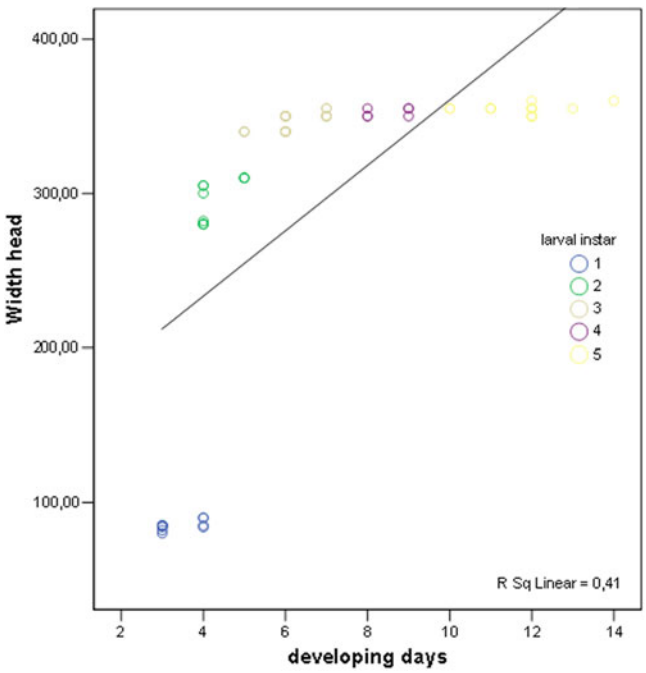

Figure 53. Scatter plot showing the relationship between the width of head, larval age, and larval instar [the fifth larva is the mature larva: predefecant mature larva + postdefecant mature larva postdefecant (prepupa)].

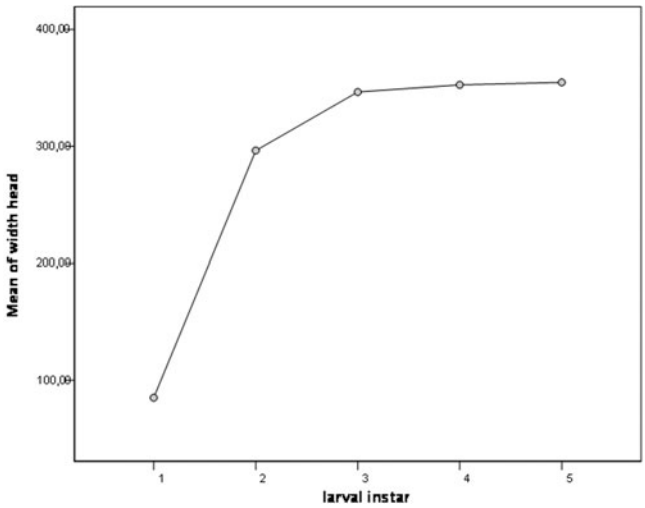

Figure 54. Relationship between head width and larval instar.

(Dyar, 1890; Odebiyi & Bokonon-Ganta, 1986; Löhr et al., 1989; Llácer et al., 2005) by authors such as Löhr et al. (1989) and Onagbola and Fadamiro (2008). These authors observed an overlap in the range of head capsule widths of different instars of *Anagyrus lopezi* (De Santis, 1964) (Hymenoptera, Encyrtidae) and *Pteromalus cerealellae* (Ashmead, 1902) (Hymenoptera, Pteromalidae), respectively. Accordingly, our results show that caution should be exercised in the use of this character to separate larval instars, and in any case mandible length, and reliable characters such as presence of exuvia should be used.

As in the case of eggs that are deposited externally, the chorion of the egg of *P. vindemmiae* is—although succinctly—sculptured (Tormos et al., 2007). Its micropylar region, as is the case of the relatively few parasitic Hymenoptera that have been reported for this structure, is at the anterior end of the egg. Although there are still very few detailed morphological studies of this region in parasitic wasps, the considerable differences between these suggest that the region may be of potential use in phylogenetic studies addressing parasitic Hymenoptera (Quicke, 1997).

The morphology of the immature larvae is similar to that reported by Crandell (1939). Nevertheless, as well as the greater detail contributed in the present work concerning the presence/absence, greater/lesser differentiation, number and position, and morphology of the different integumental and cuticular structures, it should be noted, unlike what was reported by Crandell (1939), that the labrum of the first instar does not have sensilla, and that the third instar larva has setae on the head, although smaller and more numerous than in the second instar.

The mature larva of *P. vindemmiae* shares the following character states with other Chalcidoidea: (a) reduced head, three thoracic and ten abdominal segments, and nine pair of spiracles; (b) a cephalic skeleton not very developed; and

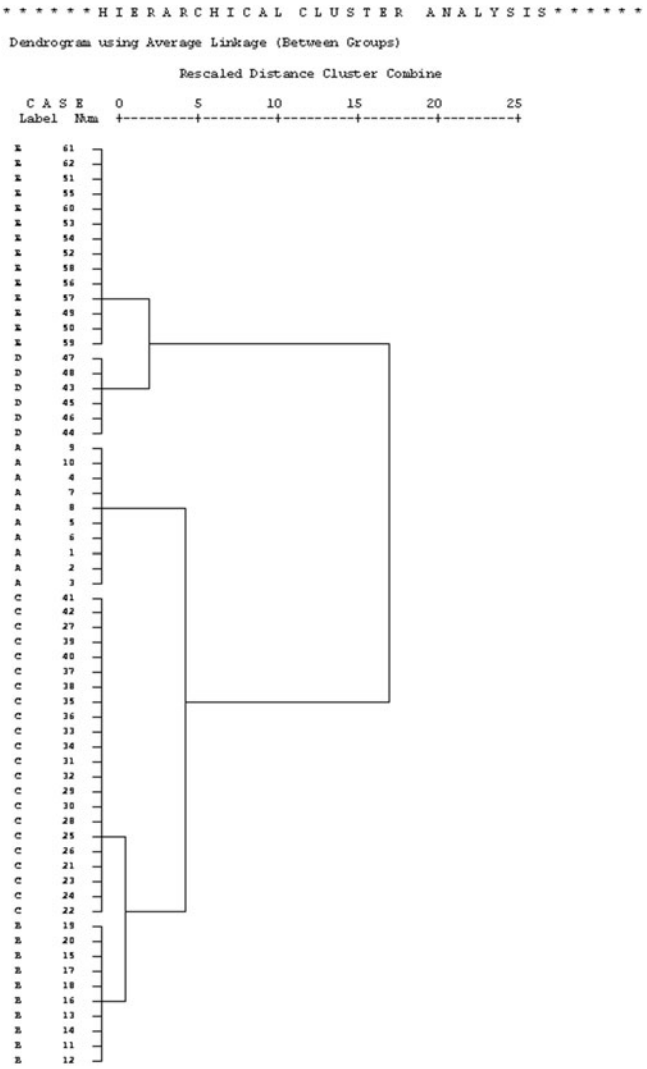

Figure 55. Dendrogram resulting from the cluster analysis using the mandible length variable (a, b, c, d, and e, correspond to the, first, second, third, fourth, and fifth larval instars, respectively).

(c) mouthparts with well-developed mandibles, sclerotized, triangular, with a short blade without teeth, and with maxillae and labium fused and salivary orifice absent.

With the mature larvae of species of Pteromalidae, it shares the presence of tubercules on some body segments as well as of a pleurostoma and superior and inferior mandibular processes. However, the presence of a completely differentiated epistoma separates this larva from known larvae of the family, and at the same time approximates it to those of *Spalangia drosophilae* (Ashmead, 1887) (Simmonds, 1953) and *S. cameroni* (Tormos et al., 2009), as well as to that of *Trichomalopsis peregrina* (Graham, 1969) (Hymenoptera, Pteromalidae) (Tormos et al., 2007). It differs from those already described in the genus in the position and number of the integumental differentations (sensilla and setae). Additionally, the distribution and number of these sensorial structures could to be important for discriminating species in the family, as occurs in the Eurytomidae (Roskam, 1982).

From the point of view of functional morphology, the mouth of the larvae, as in other ectoparasitoids, is transformed into a suctorial tube (Quicke, 1997; Llácer et al., 2005). This arrangement includes a preoral sucker, and feeding is achieved by pharyngeal pumping and continuous suction of host tissue fragments shred into tiny fragments by the mandibles (Cals-Usciati et al., 1985; Thompson, 1986; Llácer et al., 2005).

The pupa of *P. vindemmiae* was not protected by any cocoon but instead was protected inside the puparium of its host, and it had many of the features that characterize the imago, allowing its identification. Unlike the larvae, with "tusk-like" mandibles, and as in the adults, the pupa has mandibles with two apical teeth. The morphology of the pupa and the situation and morphology of the emergence hole of the adult are similar to those reported by Crandell (1939).

Although the larval instars of *P. vindemmiae* can be grossly differentiated from others species of pteromalids under a stereomicroscope (i.e., by the presence/absence and distribution of sensory structures), our results show that the eggs and different larval instars of *P. vindemmiae* can only be unambiguously identified by SEM. Accordingly, a characterization with SEM aimed at determining *a priori* the species with which one is working should precede identification routines, using a binocular microscope or stereomicroscope, for management purposes.

Acknowledgments

We are indebted to Eric Grissell (Smithsonian Institution, currently retired) for his observations and critical reading of the manuscript. María Jesús Verdú (IVIA, Spain) confirmed the determination of *P. vindemmiae*. The laboratories of the Fundación Entomológica "Torres-Sala" (Valencia, Spain) and the Servicio de Microscopía de la Universidad Politécnica de Valencia were used to carry out this study. Financial support for this article was provided from the Junta de Castilla y León, project SA012A05.

References

Bellows, T.S. & Van Driesche, R.G. (1999). Life table construction and analysis for evaluating biological control agents. In *Handbook of Biological Control. Principles and Applications of Biological Control*, Bellows, T.S. & Fisher, T.W. (Eds.), pp. 199–223. London: Academic Press.

Cals-Usciati, J., Cals, P. & Pralavorio, R. (1985). Adaptations foctionelles des structures liées à la prise alimentaire chez la larva primaire de *Trybliographa daci* Weld (Hymenoptera, Cynipoidea) endoparasite de la Mouche des fruits *Ceratitis capitata*. *C R Acad Sci III* **300**, 103–108.

Corey, S. & Reid, D.M. (1991). Comparative fecundity of decapod crustaceans. I. The fecundity of thirty tree species of nine families of caridean shrimps. *Crustaceana* **60**, 270–294.

Crandell, H. (1939). The biology of *Pahycrepoideus dubius* Ashmead (Hymenoptera). A pteromalid parasite of *Piophila case*i Linné (Diptera). *Ann Entomol Soc Am* **32**, 632–654.

Dyar, H.G. (1890). The number of moults of lepidopterous larvae. *Psyche* **5**, 420–422.

Finlaysson, T. (1987). Ichneumonoidea. In *Immature Insects*, Stehr, F.W. (Ed.), pp. 649–664. Dubuque, IA: Kendall/Hunt Publishing Company.

Geden, C.J. & Hogsette, J.A. (2006). Suppression of house flies (Diptera: Muscidae) in Florida poultry houses by sustained releases of *Muscidifurax raptorellus* and *Spalangia cameroni* (Hymenoptera: Pteromalidae). *Environ Entomol* **35**, 75–82.

Gerling, D. & Legner, E.F. (1968). Developmental history and reproduction of *Spalangia cameroni* parasite of synanthropic flies. *Ann Entomol Soc Am* **61**, 1436–1443.

Grassberger, M. & Frank, C. (2003). Temperature-related development of the parasitoid wasp, *Nasonia vitripennis* as forensic indicator. *Med Vet Entomol* **17**, 257–262.

Kawano, K. (2000). Genera and allometry in the stag beetle family Lucanidae, Coleoptera. *Ann Entomol Soc Am* **98**, 747–753.

Llácer, E., Urbaneja, A., Garrido, A. & Jacas, J. (2005). Morphology and development of immature stages of *Galleosomyia fausta* (Hymenoptera: Eulophidae: Tetrastichinae). *Ann Entomol Soc Am* **98**, 747–753.

Löhr, B., Santos, B. & Varela, A.M. (1989). Larval development and morphometry of *Epidinocarsis lopezi* (De Santis) (Hymenoptera: Encyrtidae), a parasitoid of the cassava mealybug, *Phenacoccus manihoti* Mat.-Ferr. (Homoptera: Pseudococcidae). *J Appl Entomol* **107**, 334–343.

Manzoor, F. & Akhtar, M.S. (2006). Morphometirc analysis of population samples of soldier caste of *Odontotermes obesus* (Rambur) (Isoptera, Termitidae, Macrotermitinae). *Anim Biodivers Conserv* **29**, 91–107.

Muesebeck, C.F.W. & Parker, L. (1933). *Hyposoter disparis* Viereck, and introduced ichneumonid parasite of the gypsy moth. *J Agric Res* **46**, 335–347.

Odebiyi, J.A. & Bokonon-Ganta, A.H. (1986). Biology of *Epidinocarsis* (=*Apoanagyrus*) *lopezi* (Hymenoptera: Encyrtidae) an exotic parasite of the cassava mealybug, *Phenacoccus manihoti* (Homoptera: Pseudococcidae) in Nigeria. *Entomophaga* **31**, 251–260.

Onagbola, E.O. & Fadamiro, H. (2008). Morphology and development of *Pteromalus cerealellae* (Ashmead) (Hymenoptera: Pteromalidae) on *Callosobruchus maculatus* (F.) (Coleoptera: Chrysomelidae). *BioControl* **53**, 737–750.

Protecnet (2009). Comunidad Internet para protección Fito y Zoosanitaria costarricense. Available at http://www.protecnet.go.cr/general/boletin/pleglaboratorio/plectrllbiol.htm.

Quicke, D. (1997). *Parasitic Wasps*. London: Chapmann & Hall.

Rojas-Gómez, C.V. & Bonet, A. (2003). Life cycle and development of immature stages of *Dinarmus basalis* (Rondani, 1877) (Hymenoptera, Chacidoidea: Pteromalidae). *Folia Entomol Mex* **42**, 359–370.

Roskam, J.C. (1982). Larval characters of some eurytomid species (Hymenoptera, Chalcidoidea). *Pk Ned Akad Wetensc* **85**, 293–305.

Simmonds, F.J. (1953). Parasites of the frit fly, *Oscinella frit* (L.) in eastern North America. *B Entomol Res* **43**, 503–542.

Steenberg, T., Skovgard, H. & Kalsbeek, A. (2001). Microbial and biological control of flies in stables. *DJF Rapport, Markbrug* **49**, 91–94.

Thompson, S.N. (1986). Nutrition and *in vitro* culture of insect parasitoids. *Annu Rev Entomol* **31**, 197–219.

Tormos, J., Asís, J.D., Gayubo, S.F. & Martín, M.A. (2004). Descriptions of the Final instar of *Eurytoma nodularis* and *E. heriadi* (Hymenoptera: Eurytomidae). *Fla Entomol* **87**, 278–282.

Tormos, J., Beitia, F., Böckman, E.A. & Asís, J.D. (2009). The preimaginal stages and development of *Spalangia cameroni* Perkins (Hymenoptera: Pteromalidae) on *Ceratitis capitata* (Wiedemann) (Diptera: Tephritidae). *Micron* **40**, 646–658.

Tormos, J., Frago, E., Selfa, J., Asís, J.D., Pujade, J. & Guara, M. (2007). Description of the final instar larva of *Trichomalopsis peregrina* (Hymenoptera, Pteromalidae), with data and comments on the preimaginal stages. *Fla Entomol* **90**, 180–183.

Tormos, J., Pardo, X., Jiménez, R., Asís, J.D. & Gayubo, S.F. (2003). Descriptions of adults, immature stages and venom apparatus of two new species of Dacnusini: *Chorebus pseudoasphodeli* sp. n., parasitic on *Phytomyza chaerophili* Kaltenbach and *C. pseudoasramenes* sp. n., parasitic on *Cerodontha phragmitophila* Hering (Hymenoptera: Braconidae: Alysiinae; Diptera: Agromyzidae). *Eur J Entomol* **100**, 393–400.

Tschinkel, W.R., Mikheyev, A.S. & Storz, S.R. (2003). Allometry of workers of the fire ant, *Solenopsis invicta*. *J Insect Sci* **3**, 1–11.

Wen, B., Weaver, D.K. & Brower, J.H. (1995). Size preference and sex ratio for *Pteromalus cerealellae* (Hymenoptera: Pteromalidae) in stored corn. *Environ Entomol* **24**, 1160–1166.

Wright, J.E. (1986). Immature stages of *Encyrtus saliens* (Hymenoptera: Encyrtidae), an important parasite of the ice plant scales (Homoptera: Coccidae) in California. *Ann Entomol Soc Am* **79**, 273–279.